Thin Solid Films, 25 (1975) 221–230

PIPE DIFFUSION ALONG ISOLATED DISLOCATIONS*

JÜRGEN MIMKES
Institut für Festkörperphysik, Technische Universität Berlin, 1 Berlin 12 (Germany)
(Received September 27, 1974)

The complete solution of dislocation pipe diffusion is applied to experimental data for different metals. For f.c.c. metals the mechanisms of vacancies bound to the dislocation and of diffusion in the stacking fault ribbon between dissociated dislocations are discussed. Cationic diffusion along dislocations will be obscured in the alkali halides by aliovalent impurities, but it may be observed in some metallic oxides. Anionic diffusion along dislocations may be found in all NaCl-type ionic crystals.

1. INTRODUCTION

Diffusion data will reveal information about the properties of a crystal if the right solution of the diffusion problem is applied. In order to investigate pipe diffusion along isolated dislocations, the complete solution of dislocation pipe diffusion will be applied to experimental data and will be discussed for different diffusion times. The results of the calculation enable us to discuss several mechanisms of pipe diffusion in f.c.c. metals. Similar behaviour is expected for ionic crystals with the same f.c.c. structure; however, additional effects are observed owing to the charges of the crystal and the diffusing ions.

2. APPLICATION OF THE COMPLETE SOLUTION

The complete solution of pipe diffusion along isolated dislocations for an instantaneous source[1],

$$Q(\zeta) = \gamma\,(\pi D' t)^{-1/2}\left[\exp\left(-\frac{\zeta^2}{4}\right)+\varepsilon^{1/2}\int_{1}^{\Delta}\int_{\varepsilon}^{1}\left(\frac{\zeta^2}{2\sigma}-1\right)\exp\left(-\frac{\zeta^2}{4}-\frac{\sigma-1}{\Delta-1}\,\frac{\kappa^2}{\varepsilon^2}\right)\times\right.$$

$$\left.\times\,\rho^{1/2}\,\mathrm{d}\rho\,\operatorname{erfc}\left\{\left(\frac{\Delta-1}{\Delta-\sigma}\right)^{1/2}\left(\frac{\rho-\varepsilon}{2\kappa}-\frac{\sigma-1}{\Delta-1}\,\frac{\kappa}{\varepsilon}\right)\right\}\sigma^{-3/2}\,\mathrm{d}\sigma\right] \quad (1)$$

* Paper presented at the International Conference on Low Temperature Diffusion and Applications to Thin Films, Yorktown Heights, New York, U.S.A., August 12–14, 1974.

$$\zeta = z/\sqrt{D^\ell t} \qquad \kappa = \sqrt{D^\ell t/A} = \sqrt{\pi m D^\ell t}$$

$$\Delta = D^d/D^\ell \qquad \varepsilon = a/A = \sqrt{\pi m a^2}$$

is similar to Suzuoka's solution[2] of grain boundary diffusion for an instantaneous source. ζ is the reduced bulk diffusion parameter with z the diffusion depth. Δ and ε are the pipe diffusion parameters, D^ℓ and D^d are the diffusion coefficients in bulk and pipe, respectively, a is the pipe radius and $2A$ the mean distance between the pipes. The parameter κ is determined by the dislocation density m. Applying eqn. (1) to experimental results yields the activation enthalpies h^ℓ and h^d of bulk and pipe diffusion, the diffusion constants D_0^ℓ and D_0^d of bulk and pipe diffusion, as well as the effective radius a of the dislocations if the dislocation density m is known.

2.1. $\kappa \ll 1$

For short diffusion times, $\sqrt{D^\ell t} \ll A$ (*i.e.* $\sqrt{D^\ell t}$ small compared with the mean distance $2A$ between the dislocations), the complete solution (1) may be approximated by

$$Q(\zeta) = \frac{\gamma}{(\pi D^\ell t)^{1/2}} \left\{ \exp\left(-\frac{\zeta^2}{4}\right) + \frac{\varepsilon^2}{\sqrt{\Delta}} \exp\left(-\frac{\zeta^2}{4\Delta}\right) \right\} \tag{2}$$

since the diffusion in the bulk and the pipe are still independent.

Figure 1 shows pipe diffusion data obtained by Pawel and Lundy[3], who diffused Nb into Ta for a very short time (2 h). If the logarithm of the activity is plotted against the square of the penetration depth the data points form two straight lines, referring to bulk and pipe diffusion. According to eqn. (2) the slopes will yield the bulk and pipe diffusivities D^ℓ and D^d. The value of ε may be obtained by extrapolating the straight line representing pipe diffusion to the ordinate[4]. The solid line in Fig. 1 has been calculated from the complete solution (1) and shows excellent agreement with the experimental data points. The complete solution (1) and the approximation (2) both lead to a value of ε of 0.02.

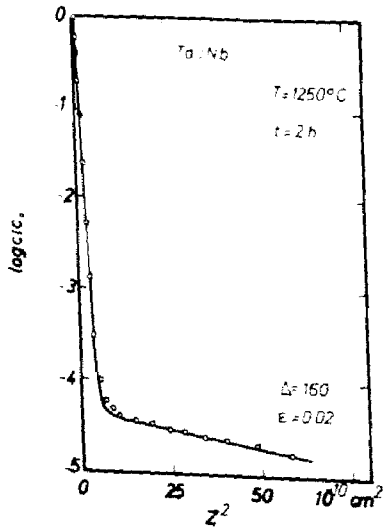

Fig. 1. Logarithm of Nb activity in Ta *vs.* the square of the penetration depth z: data points from ref. 3; solid line according to eqn. (1).

A dislocation density $m = 10^5$ cm^{-2} has been observed, and thus the effective pipe radius a may be calculated from eqn. (1): $a = \varepsilon\,(\pi\, m)^{-1/2} = 4 \times 10^{-5}$ cm. This large pipe radius may be due to the very low dislocation density m, which was determined by etching. If the real dislocation density is higher, the effective radius will become smaller.

2.2. $\kappa \leqslant 1$

For longer diffusion times, $\sqrt{D^t t} \leqslant A$, Fisher's[5] model may be applied to the dislocations, yielding Smoluchowski's solution[6]:

$$c(r,z,t) = c_0 \exp\left\{-\left(\frac{2}{\Delta a}\right)^{1/2} \frac{z}{(\pi D^t t)^{1/4}}\right\}\left(1+\frac{2}{\pi}\,\phi\right) \tag{3}$$

$$\phi = \int_0^\infty \exp\left(-\frac{D^t t\,\sigma}{a^2}\right) \frac{J_0(\sigma r/a)\, Y_0(\sigma) - J_0(\sigma)\, Y_0(\sigma r/a)}{J_0^2(\sigma) + Y_0^2(\sigma)}\,\frac{\mathrm{d}\sigma}{\sigma}$$

Figure 2 shows the self-diffusion data obtained by Reuther and Achter[7] for Nb over longer diffusion times (168 h). Two samples with different dislocation densities, which were annealed simultaneously, show the same bulk diffusivity but different pipe diffusion activities. According to eqn. (3) the logarithm of the activity c plotted against the penetration depth z will yield a straight line, from which the pipe diffusivity may be calculated. Again the solid line in Fig. 2 refers to the complete solution (1), which is in good agreement with the experimental data. The dislocation densities m(PC) $= 7.5 \times 10^5$ cm^{-2} and m(SC) $= 4 \times 10^5$ cm^{-2} yield an effective pipe radius $a = 2 \times 10^{-5}$ cm. Again the large effective pipe radius may be due to the fact that etching may not reveal all dislocations taking part in the diffusion process.

2.3. $\kappa \gg 1$

For large diffusion times, $\sqrt{D^t t} \gg A$, the bulk diffusion may be calculated according to Hart's equation[8]:

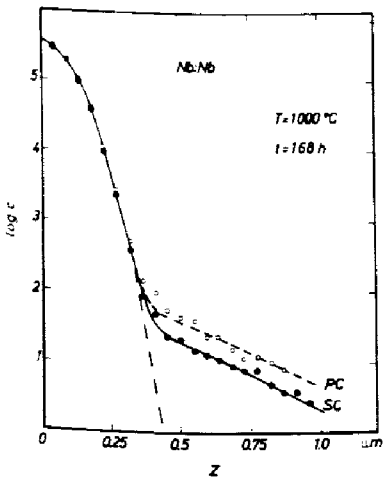

Fig. 2. Logarithm of Nb activity in Nb *vs.* the penetration depth z: data points from ref. 7; solid line according to eqn. (1).

$$Q_{\text{bulk}} = \frac{\gamma}{(\pi D_{\text{app}} t)^{1/2}} \exp\left(-\frac{z^2}{4 D_{\text{app}} t}\right) \tag{4}$$

$$D_{\text{app}} = D^{\ell} + \varepsilon^2 D^{\text{d}}$$

Figure 3 shows Gupta's data[9] for self-diffusion in gold. Gupta has calculated the bulk diffusivity according to Hart's equation (eqn. (4)) and the pipe diffusivity according to Smoluchowski's solution, since the logarithm of the activity is linear with the penetration depth z. The results for the lattice diffusivity and the product of the pipe diffusivity and the dislocation cross section are[9]

$$D_{\text{app}} = 0.07 \text{ cm}^2 \text{ s}^{-1} \exp(-1.73 \text{ eV}/kT)$$

$$\pi a^2 D_0^{\text{d}} = 5 \times 10^{-16} \text{ cm}^4 \text{ s}^{-1} \exp(-1.2 \text{ eV}/kT)$$

Again the solid lines in Fig. 3 have been calculated according to the complete solution (1).

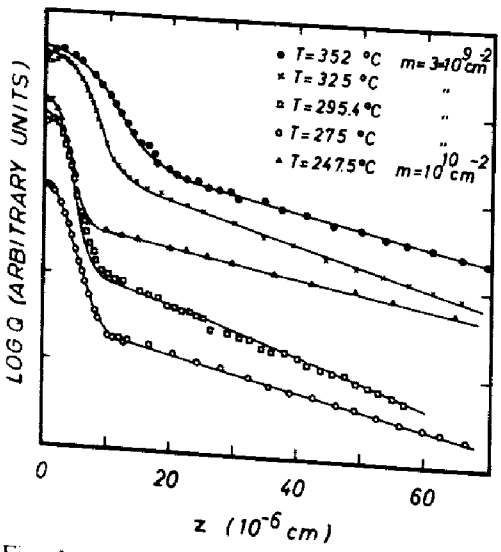

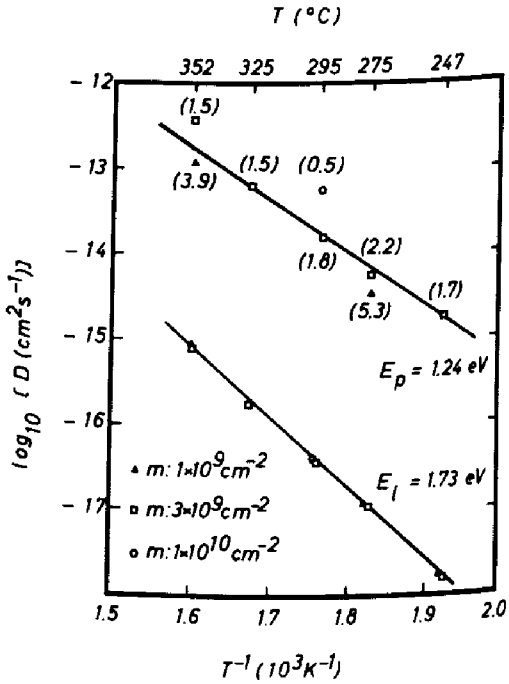

Fig. 3. Logarithm of Au activity in Au *vs.* the penetration depth z: data points from ref. 9: solid lines according to eqn. (1).

Fig. 4. Logarithm of the diffusivities for bulk and pipe self-diffusion in Au as a function of the reciprocal temperature at various dislocation densities m. Numbers for the pipe diffusion data correspond to pipe radii a (in 10^{-6} cm) calculated according to eqn. (1).

Figure 4 shows the bulk and pipe diffusivities according to the complete solution[10]. The bulk diffusivity is identical to Gupta's results:

$$D^{\ell} = 0.07 \exp(-1.73 \text{ eV}/kT) \text{ cm}^2 \text{ s}^{-1}$$

The pipe diffusivity

$$D^{\text{d}} = 2 \times 10^{-3} \exp(-1.24 \text{ eV}/kT) \text{ cm}^2 \text{ s}^{-1}$$

yields an activation enthalpy close to Gupta's value. In addition the effective dislocation radius a obtained for a fitted dislocation density $m = 3 \times 10^{9 \pm 0.5}$ cm^{-2} is $a = 1.8 \times 10^{-6 \pm 0.5}$ cm; the minimum for the effective dislocation radius according to the data is

$$a < 5 \times 10^{-7} \text{ cm}$$

which is larger by a factor of 10 than the value usually assumed.

3. PIPE DIFFUSION IN F.C.C. METALS

The results for small angle grain boundary diffusion and pipe diffusion are listed in Table I, showing the constant D_0^ℓ and enthalpy h^ℓ of bulk diffusion, the pre-exponential factor and the enthalpy of pipe diffusion, the Burgers vector $\boldsymbol{b}$ of the dislocations involved and the impurity content of the specimen. The data do not seem to depend on the impurity concentration; the type of dislocation may have some influence, however. In order to compare the results for grain boundary diffusion and pipe diffusion, the pre-exponential factor P_0^d of dislocations in the grain boundary has been calculated from the angle θ and the width δ of the grain boundary[11, 18]:

$$P_0^d = \pi a^2 D_0^d = \frac{\delta^2 D_0^d}{2 \sin(\theta/2)} \tag{5}$$

Three simple models will be discussed in more detail in order to explain the observed activation enthalpies and pre-exponential factors for pipe diffusion.

3.1. *Vacancies bound in the stress field of dislocations*

Balluffi[18] has discussed the model of vacancies bound in the stress field of the dislocation. In this model the expected radius of the dislocation should be of

TABLE I

SELF-DIFFUSION ALONG DISLOCATIONS IN F.C.C. METALS

Element	D_0^ℓ (cm^2 s^{-1})	h^ℓ (eV)	*Pre-exponential factor*	h^d (eV)	$\boldsymbol{b}$	*Impurities* (ppm)	*Ref.*
Ag	0.25	1.95	$\delta D_0^d = 2 \times 10^{-10}$ cm^3 s^{-1}	0.86	[100] edge	200	11
Ag	0.395	1.92	$ma^2 D_0^d = 6 \times 10^{-5}$ cm^2 s^{-1}	1.30		10	12
Ag	0.44	1.92	$\delta D_0^d = 3 \times 10^{-11}$ cm^3 s^{-1}	0.51	[100] edge	1	13
Ag	0.44	1.92	–	1.30	[112] edge	1	13
Au	0.091	1.81	$\pi a^2 D_0^d = 5 \times 10^{-16}$ cm^4 s^{-1}	1.20	[110] edge	10	9
			$D_0^d = 0.002$ cm^2 s^{-1}	1.24	[110] edge	10	10
			$a = 5 \times 10^{-7}$ cm				
Al	0.18	1.31	$\pi a^2 D_0^d = 7 \times 10^{-17}$ cm^4 s^{-1}	0.85	[110] edge	1	14
Ni	1.9	2.89	$\delta D_0^d = 5 \times 10^{-11}$ cm^3 s^{-1}	1.08	[100] edge	500	15
Ni	1.9	2.89	$D_0^d = 20$ cm^2 s^{-1}	1.6	[110] edge	10	16
			$a = 2 \times 10^{-7}$ cm				
Ni	1.9	2.89	$\delta D_0^d = 8 \times 10^{-8}$ cm^3 s^{-1}	1.76	[110] edge	300	17
Ni	1.9	2.89	$\delta D_0^d = 5 \times 10^{-8}$ cm^3 s^{-1}	1.95	[110] screw	300	17

the order of the Burgers vector, 5 Å. The activation enthalpy of pipe diffusion is[18]

$$h^{d} = h_{f}^{f} + h_{m}^{d} + h_{b}^{d}$$

where h_f^f is the enthalpy of formation in the bulk, h_m^d the enthalpy of migration near the dislocation, and h_b^d the (negative) binding enthalpy to the dislocation. If the enthalpy of migration near the dislocation is assumed to be the same as that in the bulk, very large (and unreasonable) binding enthalpies are obtained. Lothe[19] has suggested a more reasonable value of 0.5 h_m^f for h_m^d. Table II shows the experimental results for dislocation pipe diffusion in f.c.c. metals and the calculated enthalpies. Diffusion along undissociated [100] dislocations still reveals large binding enthalpies h_b^d; the product $P_0^d = a^2\ \pi\ D_0^d \approx 10^{-18}$ cm^4 s^{-1} indicates a small pipe radius a. Diffusion along dissociated [110] dislocations shows very reasonable binding enthalpies of the order of a few tenths of an electron volt. However, the pre-exponential factor P_0^d is much larger than the equivalent values for undissociated dislocations. Thus the model of vacancies bound in the stress field of dislocations yields unexpectedly large binding enthalpies for diffusion along undissociated dislocations; along dissociated dislocations the effective

TABLE II

MODEL OF A VACANCY BOUND TO A DISLOCATION BY THE STRESS FIELD

$h^d = h_f^f + h_m^d + h_b^d$

Element	h^d (eV)	h_f^f (eV)	$h_m^d = \frac{1}{2} h_m^f$ (eV)	h_b^d (eV)	P_0^d (cm^4 s^{-1})	*b*	*Ref.*
Ag	0.86	1.10	0.40	−0.64	5.2×10^{-17}	[100]	11
Ag	0.51	1.10	0.40	−0.99	4.7×10^{-18}	[100]	13
Ni	1.08	1.9	0.5	−1.32	9.3×10^{-18}	[100]	15
Al	0.85	0.76	0.3	−0.21	7×10^{-17}	[110]	14
Ni	1.6	1.9	0.5	−0.8	5.6×10^{-12}	[110]	16
Ni	1.75	1.9	0.5	−0.65	3.1×10^{-15}	[110]	17
Ni	1.95	1.9	0.5	−0.45	6.6×10^{-15}	[110]	17
Ag	1.3	1.1	0.4	−0.2	$> 1 \times 10^{-15}$	[110]	12
Ag	1.30	1.10	0.40	−0.2	–	[112]	13
Au	1.2	0.98	0.41	−0.2	5×10^{-16}	[110]	9

radius of the dislocations appears to be higher than that ordinarily assumed for this model.

3.2. *Vacancy mechanism*

A constant vacancy mechanism of pipe diffusion requires an enthalpy of migration only:

$$h^{d} = h_{m}^{d}$$

where h_m^d is expected to be less than or equal to the enthalpy of migration in the bulk h_m^f. According to Table III this model may be applied for diffusion along [100] dislocations, where

$$h^d \leqslant h_m^\ell$$

has been found to hold for self-diffusion in silver and nickel.

TABLE III

VACANCY MODEL FOR UNDISSOCIATED DISLOCATIONS AND MODEL OF PIPE DIFFUSION IN THE STACKING FAULT RIBBON OF DISSOCIATED DISLOCATIONS

Element	h^d (eV)	h_m^ℓ (eV)	P_0^d (cm^4 s^{-1})	d (Å)	*b*	*Ref.*
Ag	0.86	0.81	5.2×10^{-17}	–	[100]	11
Ag	0.51	0.81	4.7×10^{-18}	–	[100]	13
Ni	1.08	1.0	9.3×10^{-18}	–	[100]	15
Al	0.85	0.6	7×10^{-17}	7.5	[110]	14
Ni	1.6	1.0	($a = 20$ Å)	11	[110]	16
Ni	1.75	1.0	3.1×10^{-15}	11	[110]	17
Ni	1.95	1.0	6.6×10^{-15}	11	[110]	17
Ag	1.3	0.81	1×10^{-15}	34	[110]	12
Ag	1.3	0.81	–	34	[112]	13
Au	1.2	0.83	($a = 50$ Å)	34	[110]	9,10

The small pre-exponential factor P_0^d for [100] dislocations indicates a small pipe radius of one or two Burgers vectors. Lothe[19] has shown that only a few strings of atomic jump positions are needed to obtain a sufficiently large correlation factor. Thus a vacancy mechanism is in good agreement with the diffusion data for [100] dislocations.

3.3. *Dissociated dislocations*

In contrast to dislocations with [100] Burgers vectors the [110] dislocations may dissociate into partials; thus a different diffusion mechanism is to be expected. Indeed, a vacancy mechanism cannot be applied to [110] dislocations since the observed activation enthalpy of pipe diffusion h^d is larger than the enthalpy of migration in the bulk h_m^ℓ in all samples listed in Table III. In addition, the calculated pre-exponential factors P_0^d, as well as the calculated pipe radii a, grow in proportion to the spacing d between the partials, as shown in the third and fourth columns of Table III. The area of the dislocation pipes is of the order of the width of the stacking fault ribbon, indicating a mechanism of enhanced diffusion in the stacking fault ribbon. The stacking fault is represented by an area with h.c.p. structure enclosed in the f.c.c. metal. Thus the spring constant of the second nearest neighbours in the ribbon differs from that in the bulk, giving rise to a new attack frequency in the ribbon:

$$\nu' = \nu_D' \exp(-h_m'/kT)$$

where ν_D' is a vibrational mode of the stacking fault ribbon and h_m' is the enthalpy of migration in the ribbon. This may explain the large area calculated for pipe diffusion along [110] dislocations, since the vibrational mode will not be confined to the dislocation cores of the partials but will apply to the complete stacking fault ribbon. The activation enthalpy observed for pipe diffusion along [110]

dislocations is also in the range to be expected: it should be less than that in the bulk and larger than that in the highly perturbed area of [100] dislocations.

Love[20] and Wever *et al.*[21] have discussed different models, but more experimental data, including the accurate determination of the dislocation density, will be needed to confirm and explain the large effective pipe radii for diffusion along dissociated dislocations.

4. PIPE DIFFUSION IN IONIC CRYSTALS

The diffusion coefficient of intrinsic cation and anion diffusion is given by

$$D^{\text{intr}} = \gamma \lambda^2 \nu_D f \exp\left(-\frac{g_f}{kT} - \frac{g_m}{kT}\right) \tag{6}$$

with γ the geometrical factor, λ the jumping width, ν_D the Debye frequency, f the correlation factor, g_f the free enthalpy of formation and g_m the free enthalpy of motion. For extrinsic diffusion the diffusion coefficient is

$$D^{\text{extr}} = \gamma \lambda^2 \nu_D f n_v \exp\left(-\frac{g_m}{kT}\right) \tag{7}$$

where n_v is the concentration of vacancies due to aliovalent impurities. Extrinsic diffusion will occur for temperatures below T_0, where T_0 is given by

$$n_v = n_i = \exp\left(-\frac{g_f}{kT_0}\right) \tag{8}$$

if the extrinsic cation diffusion in NaCl is due to a concentration n_i of Ca^{2+}. The temperature T_0 depends only on the concentration n_i of Ca^{2+}:

$$T_0 = \frac{h_f}{s_f - k \ln n_i} \tag{9}$$

Above T_0 only intrinsic bulk diffusion will be observed.

Cationic pipe diffusion may occur in both the intrinsic and the extrinsic temperature ranges. In order to observe enhanced cationic pipe diffusion in the intrinsic range, the lower boundary of the (normalized) intrinsic range

$$1 = T_m/T_m \geq T/T_m \geq T_0/T_m$$

must be as low as possible. Table IV shows T_0, calculated according to eqn. (9) for a doping level of 1 ppm, for several ionic crystals. The free enthalpy of vacancy formation and the melting temperature are also indicated in the table. For alkali halides T_0 is about 70% of the melting temperature T_m, whereas T_0 is less than 50% of T_m for MgO.

In order to obtain an intrinsic temperature range

$$1 \geq T/T_m \geq 0.5$$

in alkali halides as well, the maximum impurity concentration n_i of Ca^{2+} has been calculated from eqn. (8) and is given in the sixth column of Table IV.

TABLE IV

KNEE TEMPERATURE T_0 FOR AN ALIOVALENT IMPURITY CONCENTRATION OF 1 ppm AND THE MAXIMUM ALLOWED CONCENTRATION n_i OF ALIOVALENT IMPURITIES FOR THE OBSERVATION OF CATIONIC PIPE DIFFUSION IN THE INTRINSIC RANGE OF IONIC CRYSTALS

MX	s_f/k	h_f (eV)	T_m (K)	T_0 (n_i = 1 ppm)	$n_i(0.5\,T_m)$ (ppm)	*Ref.*
K Br	5.0	1.18	1003	0.73 T_m	2.3×10^{-4}	22
K Cl	3.8	1.16	1049	0.73 T_m	3.6×10^{-4}	22
Na Cl	3.1	1.06	1073	0.68 T_m	2.4×10^{-3}	22
Na Cl	6.1	1.07	1073	0.66 T_m	4×10^{-2}	23
Mg O	0.9	1.9	3073	0.49 T_m	1.4	24

The calculated concentrations in Table IV reveal that it will be difficult to observe enhanced diffusion of cations along dislocations in the intrinsic range for the alkali halides because it will most probably be obscured by extrinsic diffusion. Owing to the high melting temperature, however, it may be possible to observe cationic diffusion along dislocations in MgO and other metal oxides in the intrinsic range. Table V shows experimental results for cationic and anionic diffusion in ionic crystals. No enhanced diffusion is observed for cationic diffusion

TABLE V

CATIONIC AND ANIONIC DIFFUSION ALONG DISLOCATIONS IN IONIC CRYSTALS

MX : El	D_0' (cm^2 s^{-1})	h' (eV)	*Pre-exponential factor*	h^d (eV)	*Ref.*
Na Cl : Na^+	1×10^{-6}	0.8	–	0.8	25
Mg O : Co^{2+}	5.8×10^{-5}	2.05	–	2.05	26
: Ni^{2+}	1.2×10^{-5}	2.1	–	2.1	26
: Ni^{2+}	6×10^{-6}	1.8	–	1.8	27
Mg O : Ba^{2+}	0.07	3.38	$ma^2D_0^d = 6\times10^{-5}$ cm^2 s^{-1}	1.85	28
Th O_2 : Th^{2+}	0.35	6.48	$\delta D_0^d = 8\times10^{-14}$ cm^3 s^{-1}	2.1	29
Na Cl : Na^+	6×10^{-4}	1.23	–	0.4	30
K Br : Br^-	3×10^{4}	2.61	$\delta D_0^d = 7\times10^{-13}$ cm^3 s^{-1}	1.49	31
Na Cl : I^-	5×10^{2}	2.27	$\delta D_0^d = 8.5\times10^{-5}$ cm^3 s^{-1}	1.36	32

in NaCl or Co^{2+} and Ni^{2+} diffusion in MgO: the activation enthalpies for bulk and pipe diffusion are identical and the activation enthalpy as well as the diffusion constant D_0' of bulk diffusion indicate an extrinsic mechanism. Only for Ba^{2+} diffusion in MgO and for Th^{2+} in ThO_2 has diffusion enhancement along dislocations been observed: the coefficients of bulk diffusion point to an intrinsic mechanism.

In order to observe enhanced cationic pipe diffusion in alkali halides, a very low temperature in the extrinsic range of highly pure crystals has to be chosen. In this temperature range associates are formed, yielding a higher activation enthalpy of diffusion than in the impurity-controlled range, and pipe diffusion may be observable. Recent results for NaCl and KBr indicate that enhanced

cationic diffusion along dislocations may indeed be found at very low temperatures in the extrinsic range of alkali halides of ultrahigh purity ($n_i < 1$ ppm)[30].

Since anionic diffusion is not affected in the same way as cationic diffusion by aliovalent cation impurities, enhanced diffusion of anions along dislocations may be observed in both metal oxides and alkali halides. This is shown by the results for NaCl and KBr in Table V. At present no pipe diffusion mechanism is offered for ionic crystals, since more data will be needed to draw further conclusions.

ACKNOWLEDGEMENTS

I would like to thank Professor A. D. Le Claire, Professor R. W. Balluffi and Professor M. Wuttig for helpful discussions.

REFERENCES

1 J. Mimkes and M. Wuttig, *Phys. Rev., B2* (1970) 1619.
2 T. Suzuoka, *J. Phys. Soc. Japan, 19* (1964) 839.
3 R. E. Pawel and T. S. Lundy, *Acta Met., 13* (1965) 345.
4 J. Mimkes, *Phys. Status Solidi (b), 58* (1973) K31.
5 J. C. Fisher, *J. Appl. Phys., 22* (1951) 74.
6 R. Smoluchowski, *Phys. Rev., 87* (1952) 482.
7 T. C. Reuther and M. R. Achter, *Met. Trans., 1* (1970) 1777.
8 E. W. Hart, *Acta Met., 5* (1957) 597.
9 D. Gupta, *Phys. Rev., B7* (1973) 586.
10 J. Mimkes, *Phys. Rev., B9* (1974) 5320.
11 D. Turnbull and R. E. Hoffmann, *Acta Met., 2* (1954) 419.
12 C. T. Lai and H. M. Morrison, *Can. J. Phys., 48* (1970) 1548.
13 J. T. Robinson and N. L. Peterson, *Surface Sci., 31* (1972) 586.
14 T. E. Volin and R. W. Balluffi, *Appl. Phys. Letters, 11* (1967) 259.
15 W. R. Upthegrove and M. J. Sinnot, *Trans. ASM, 50* (1958) 1031.
16 M. Wuttig and K. Birnbaum, *Phys. Rev., 147* (1966) 495.
17 R. F. Cannon and J. P. Stark, *J. Appl. Phys., 40* (1969) 4361.
18 R. W. Balluffi, *Phys. Status Solidi, 42* (1970) 11.
19 J. L. Lothe, *J. Appl. Phys., 31* (1960) 1077.
20 G. R. Love, *Acta Met., 12* (1964) 731.
21 H. Wever, P. Adam and G. Frohberg, *Acta Met., 16* (1968) 1289.
22 P. Süppitz and J. Teltow, *Phys. Status Solidi, 23* (1967) 9.
23 K. L. Kliewer and J. S. Koehler, *Phys. Rev., 157* (1967) 685.
24 B. C. Harding and D. M. Price, *Phil. Mag., 26* (1972) 253.
25 K. R. Riggs and M. Wuttig, *J. Appl. Phys., 40* (1969) 4682.
26 B. J. Wuensch and T. Vasilos, *J. Amer. Ceram. Soc., 49* (1966) 433.
27 J. Mimkes and M. Wuttig, *J. Amer. Ceram. Soc., 54* (1971) 65.
28 B. C. Harding, *Phil. Mag., 16* (1967) 1039.
29 A. D. King, *J. Nucl. Mater., 38* (1971) 347.
30 J. L. Schlederer, *Thesis*, Univ. of New South Wales, Australia, 1974.
31 D. K. Dawson and L. W. Barr, *Proc. Brit. Ceram. Soc., 9* (1967) 171.
32 K. S. Sabharwal, J. Mimkes and M. Wuttig, in preparation.